Study on Mechanical Properties of Sandstone Under the Coupling Effects of Cyclic Loading and Acid-Alkali Erosion

Zihao Zhu, Yu Yang*, Shunyi Wang

School of Civil Engineering, Liaoning Technical University, Fuxin 123000, China

*Correspondence Email Address: 2414275270@qq.com

Abstract. To examine the damage evolution of fine sandstone under combined cyclic loading and acid–base erosion, sandstone from Daming Coal Mine was tested under different stress-upper limits and multi-pH solutions. Damage variables D_a (energy-based) and D_b (porosity-based) were defined. Results show D_a grows with cycle number at a decelerating rate, and increases with higher stress limits. D_b follows acidic > alkaline > neutral under the same pH, and rises with prior loading amplitude. The study clarifies coupled damage mechanisms, offering a basis for assessing abandoned-mine roadway stability.

Keywords: Fine sandstone, Cyclic loading, Acid-base erosion, Damage evolution

1 Introduction

The surrounding rock of coal mine roadways is subjected to a complex coupled environment of repeated mining-induced stress disturbances and chemical erosion from mine water throughout its entire life cycle, particularly during the later stages of mine service and after abandonment. Frequent cyclic loading leads to fatigue damage and crack accumulation within the surrounding rock, a process that has been extensively documented in previous studies. Fuenkajorn et al. observed an exponential decay in the strength of rock salt with increasing number of cycles[1], Bagde et al. investigated the influence of loading frequency and amplitude on the fatigue performance of sandstone[2], Liu et al. developed a damage constitutive model based on energy dissipation[3], and domestic scholar Ge Xiurun et al. experimentally confirmed the stress threshold characteristic of rock fatigue failure.

Simultaneously, groundwater rich in various ions, especially acidic or alkaline mine water, further weakens the bonding between mineral particles through dissolution, ion exchange, and other water–rock chemical interactions. Feng et al. utilized real-time CT imaging to observe the damage evolution in sandstone under chemical corrosion[4], Qiao et al. systematically studied how hydro-physicochemical effects alter the mesoscopic properties and mechanical behavior of sandstone[5], and Li et al. quantitatively reported the reduction in uniaxial compressive strength of sandstone due to acid

© The Author(s) 2026
S. Sing et al. (eds.), *Proceedings of the 2025 7th International Conference on Civil Architecture and Urban Engineering (ICCAUE 2025)*, Atlantis Highlights in Engineering 43,
https://doi.org/10.2991/978-94-6239-682-1_26

corrosion[6]. Additionally, the influence of moisture content itself on the mechanical properties of rock cannot be overlooked[7–8], and research on the damage mechanisms of acidic chemical solutions has been extended to materials such as granite[9].

These mechanical and chemical processes interact synergistically, collectively exacerbating the deterioration of the mechanical performance of surrounding rock. This represents a critical scientific challenge in the resource utilization and safety assurance of abandoned mines[10]. However, existing research has predominantly focused on the effects of individual factors. Currently, there is still a lack of quantitative characterization of damage variables, the evolution laws of damage, and research on the coupling of "mechanical loading - chemical erosion" sequence, especially for the roof sandstone with specific mineral composition.

This study designs systematic cyclic loading-unloading and multi-pH erosion tests, defining mechanical D_a (energy-based) and D_b (porosity-based) damage variables to reveal damage evolution and failure mechanisms in fine sandstone under coupled conditions, providing a theoretical basis for assessing long-term stability and disaster prevention in abandoned mine roadways.

2 Experiment

2.1 Sandstone Materials

The fine sandstone specimens used in this study were obtained from the roadway roof at a depth of approximately 600 m in the Daming Coal Mine, Liaoning. They exhibit a grayish-white color, fine-grained texture, and uniform structure. Following the International Society for Rock Mechanics (ISRM) standards, the samples were machined into standard cylindrical specimens measuring 50 mm in diameter and 100 mm in height (Fig. 1). The mineral composition of the rock samples, as determined by X-ray diffraction (XRD) whole-rock mineral analysis, is shown in Fig. 2. The composition includes quartz (49.2%), plagioclase (30.4%), potassium feldspar (11.4%), chlorite (4.2%), illite (3.8%), and talc (1.0%).

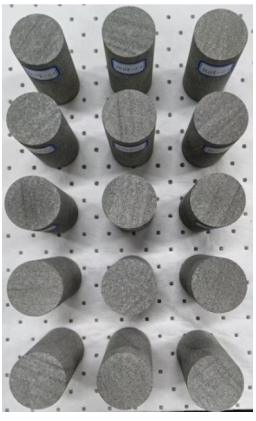

Fig. 1. Sandstone sample

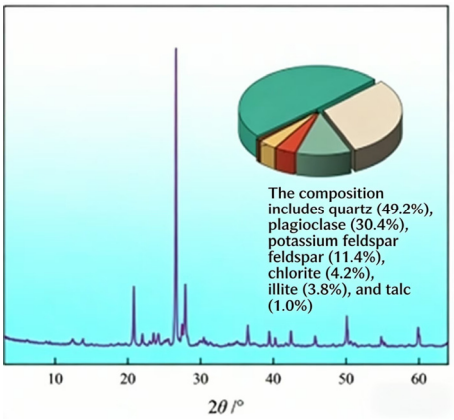

Fig. 2. XRD mineral analysis results

2.2 Cycling Loading Test

Rock specimens with different damage levels were prepared through uniaxial cyclic loading-unloading tests. The results show that the average uniaxial compressive strength of this fine sandstone is approximately 77.8 MPa, and the failure mode is dominated by shear failure (Fig. 3). Set the lower limit $\sigma_{\min}$ uniformly to 15 MPa (19% σ_c), and set the upper limits $\sigma_{\max}$ to 25 MPa (32% σ_c), 35 MPa (45% σ_c), and 45 MPa (58% σ_c) respectively.

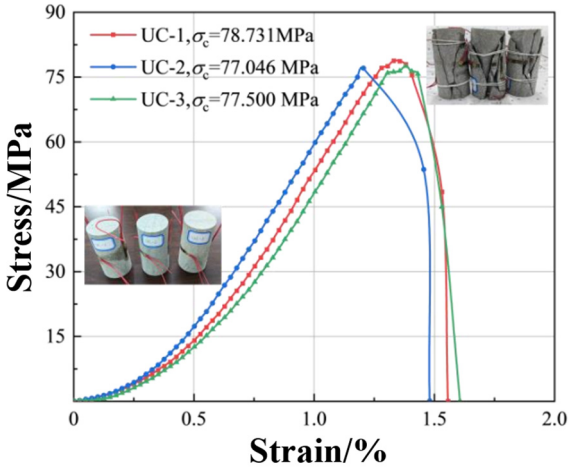

Fig. 3. The stress-strain curve of sandstone

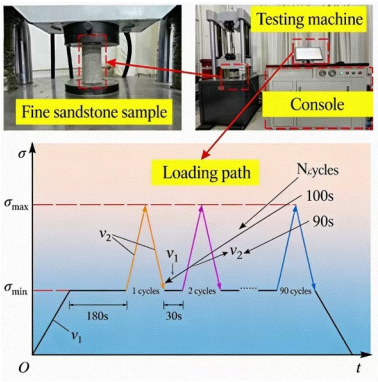

Fig. 4. Cycling Loading Test

Thirty sandstone specimens were evenly divided into three groups: PA, PB, and PC. The test was conducted under stress control: first, loaded to σ_{min} at a rate of 0.5 kN/s and held for 180 s. Subsequently, they were loaded to the corresponding $\sigma_{\max}$ at 1.0 kN/s and immediately unloaded back to σ_{min}, followed by a 30 s hold period—this entire process was defined as one cycle. Each group underwent 50 such cycles. Finally, all specimens were unloaded to zero at a rate of 0.5 kN/s (Fig. 4).

3 Experimental Results

Fig. 5 shows typical stress-strain curves of sandstone during cyclic loading-unloading under different upper stress limits. It can be observed that the hysteresis loops evolve from sparse to dense as the number of cycles increases, indicating that the growth rate of dissipated energy in the rock specimen gradually decreases with progressive cycling.

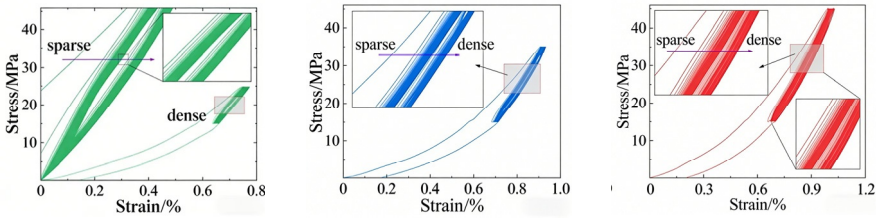

Fig. 5. Stress-strain curves of sandstone under different loading limits

To quantify the damage degree of sandstone under cyclic loading, a damage variable is defined based on the ratio of dissipated energy to constitutive energy:

$$D_a = U_d/U \tag{1}$$

where D_a is the damage variable induced by cyclic loading, in kJ; U_d is the dissipated energy during cyclic loading-unloading, in kJ; and U is the constitutive energy during uniaxial compression, in kJ.

Based on the above equation, the damage variable D_a for each rock specimen and the average damage variable were obtained, as shown in Table 1.

Table 1. Damage variable D_a of sandstone under cyclic loading

Sample grouping	Dissipated energy $U_d\ /kJ$	Average constitutive energy U/kJ	Damage variable D_a	Average damage variable
PA	3.99388	104.6263	0.038173	0.0382202
	3.92520		0.037516	
	4.00860		0.038314	
	4.01336		0.038359	
	3.98365		0.038075	
	3.99495		0.038183	
	3.95916		0.037841	
	4.04307		0.038643	
	4.00546		0.038284	
	4.06100		0.038814	
PB	6.69487		0.063988	0.0635694
	6.71430		0.064174	
	6.58399		0.062929	
	6.73772		0.064398	
	6.59554		0.063039	
	6.52115		0.062328	
	6.80029		0.064996	
	6.60045		0.063086	
	6.72549		0.064281	
	6.53650		0.062475	
PC	10.47170		0.100087	0.1007816
	10.54216		0.100760	
	10.54549		0.100792	
	10.61580		0.101464	
	10.49193		0.100280	
	10.58452		0.101165	
	10.49559		0.100315	
	10.53419		0.100684	
	10.65330		0.101822	
	10.50938		0.100447	

To characterize the evolution of damage during cyclic loading-unloading, the damage evolution coefficient ψ_n is defined as the ratio of the dissipated energy W_d^n in the n-th cycle to the total dissipated energy W_d^{50} after completing all cycles. The damage variable D_a^n after the n-th cycle can then be expressed as:

$$\psi_n = W_d^n / W_d^{50} \tag{2}$$

$$D_a^n = \psi_n D_a \tag{3}$$

The results are shown in Fig. 6. As the number of cycles increases, the damage variable gradually increases, but its growth rate progressively slows down. Meanwhile, under the same number of cycles, a higher upper stress limit leads to a larger damage variable value and a faster growth rate.

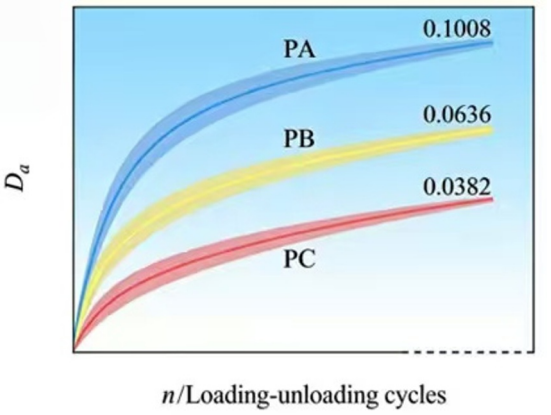

Fig. 6. Curve showing the variation of damage variable D_a with the number of cyclic loading and unloading cycles

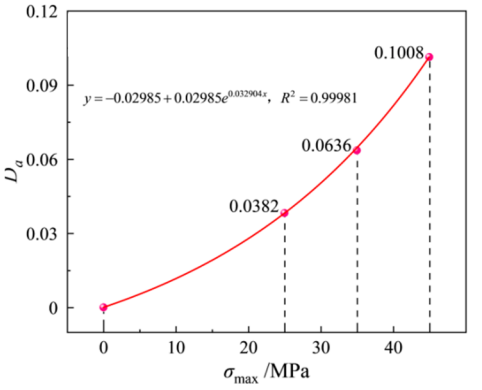

Fig. 7. The fitted curve of the damage variable D_a with respect to the upper limit of stress loading

Through fitting the upper stress limit against the average damage variable, an exponential relationship between the two was identified (Fig. 7). When the upper stress limit increased from 25 MPa to 35 MPa, the increment in the damage variable was 0.0253; when further increased to 45 MPa, the increment rose to 0.0372, with a growth rate of 46.8%.

4 Acid and Alkali Erosion Treatment

To simulate the influence of water–rock interactions on the mechanical properties of sandstone in a mine water environment, solutions with pH values of 4, 5, 6, 7, and 8, as well as a salt solution with a mineralization degree of 1 g/L, were prepared. The treatment of the acid-base erosion process includes deionized water, sealing treatment, and complete immersion of the rock samples. The experimental procedure is illustrated in Fig. 8.

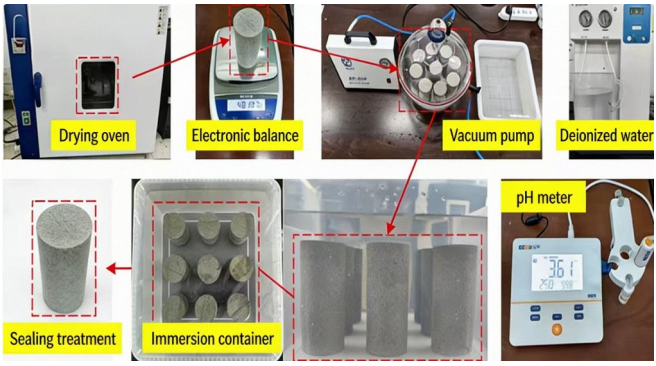

Fig. 8. Process of Acid and Alkali Erosion Treatment

4.1 Analysis of Acid and Alkali Erosion Results

During the 65-day acid–base erosion test, the pH of the solutions was monitored daily to track the progress of chemical erosion (Fig. 9). Under acidic conditions, the pH gradually approached the set value and stabilized, indicating that the reaction between H^+ and minerals slowed as the reactants were consumed. Under neutral conditions, the pH fluctuated slightly within the range of 7.00–7.08, and the solution became turbid. Under alkaline conditions, minor pH fluctuations occurred in the initial stage, reflecting limited reactions between OH^- and minerals, and the pH later stabilized at pH=8.0.

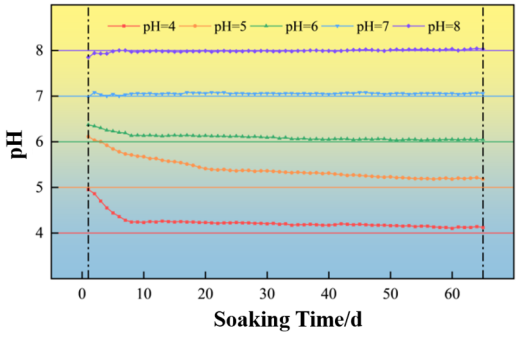

Fig. 9. Daily pH value changes in different solutions

Since sandstone is a clastic sedimentary rock, its mechanical properties are primarily influenced by the mechanical characteristics and microstructure of the solid mineral particles and the cementing material between them. The porosity and damage variable D_b of the rock specimens after 65 days of immersion in solutions with different pH levels are presented in Table 2.

Table 2. Damage Variables D_b of Sandstone under Acidic and Alkaline Erosion

Specimen number	Porosity before hydrothermal alteration ϕ_0/%	Porosity after hydrothermal action ϕ_0/%	Secondary porosity ϕ'/%	Average damage variable D_b
PA-H4	3.559	4.635	1.076	0.011157
	3.331	4.410	1.079	
PA-H5	3.249	4.314	1.065	0.011008
	3.396	4.459	1.063	
PA-H6	3.287	4.344	1.057	0.010929
	3.354	4.410	1.056	
PA-H7	3.111	4.045	0.934	0.009640
	3.258	4.191	0.933	
PA-H8	3.230	4.185	0.955	0.009869
	3.191	4.146	0.955	
PB-H4	3.175	4.258	1.083	0.011185
	3.235	4.317	1.082	
PB-H5	3.124	4.195	1.071	0.011055
	3.165	4.236	1.071	
PB-H6	3.103	4.165	1.062	0.010960
	3.323	4.383	1.060	
PB-H7	3.074	4.016	0.942	0.009719
	3.448	4.386	0.938	
PB-H8	3.444	4.405	0.961	0.009953
	3.234	4.197	0.963	
PC-H4	3.202	4.293	1.091	0.011271
	3.369	4.458	1.089	
PC-H5	3.356	4.437	1.081	0.011185
	3.124	4.208	1.084	
PC-H6	3.223	4.293	1.070	0.011056
	3.256	4.326	1.070	
PC-H7	3.470	4.421	0.951	0.009852
	3.146	4.100	0.954	
PC-H8	3.389	4.361	0.972	0.010061
	3.378	4.350	0.972	

Based on the acid–base erosion test results (Fig. 10), the damage variable of sandstone varies significantly with the pH of the solution: the average damage variable is 0.011204 at pH = 4 and decreases to 0.009737 at pH = 7. Under the same cyclic loading history and mineralization degree, the damage degree follows the order:

acidic > alkaline > neutral. Moreover, under the same pH condition, the damage variable increases with the amplitude of the prior cyclic loading (25 MPa < 35 MPa < 45 MPa). High loads will increase the number of micro-cracks, exposing the surfaces and interfaces of the hydration products that are not in contact with the surrounding medium, and reducing the resistance of the erosion medium to penetration, allowing it to penetrate deeper into the material. Together, these actions expand the effective reaction interface for chemical erosion.

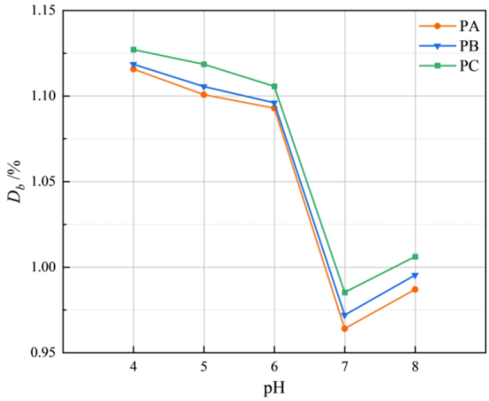

Fig. 10. Damage variable D_b of rock samples after immersion in different solutions

5 Conclusion

Based on the pre-damage tests of fine sandstone under cyclic loading and acid-base erosion, the damage degree of the pretreated sandstone was quantitatively evaluated by introducing damage variables according to the variations in dissipated energy under cyclic loading and the evolution of porosity after acid-base erosion. The main conclusions are as follows:

(1) The damage variable D_a calculated based on the energy method shows that for a single specimen, the damage variable increases with the growing number of cycles, while the growth rate gradually slows down; for different specimens, under the same number of cycles, a higher upper stress limit results in a larger damage variable value and a faster growth rate.

(2) The damage variable Db calculated based on the secondary porosity of the rock specimens indicates that the effect of pH on the degree of damage follows the order: acidic > alkaline > neutral. Under the same pH condition, the damage variable increases with the rise of the upper cyclic loading limit from the previous test, following the pattern: 25 MPa < 35 MPa < 45 MPa.

(3) There exists a significant coupling effect between cyclic loading and acid–base erosion. Microcracks induced by prior mechanical damage enlarge the reactive interface for chemical erosion, which further aggravates the damage and deterioration of the fine sandstone.

References

1. Fuenkajorn K, Phueakphum D. Effects of cyclic loading on mechanical properties of Maha Sarakham salt[J]. Engineering Geology, 2010, 112(1-4): 43-52.
2. Bagde M N, Petroš V. Fatigue properties of intact sandstone samples subjected to dynamic uniaxial cyclical loading[J]. International Journal of Rock Mechanics and Mining Sciences, 2005, 42(2): 237-250.
3. Liu X S, Ning J G, Tan Y L, et al. Damage constitutive model based on energy dissipation for intact rock subjected to cyclic loading[J]. International Journal of Rock Mechanics and Mining Sciences, 2016, 85: 27-32.
4. Feng X T, Chen S L, Zhou H. Real-time computerized tomography (CT) experiments on sandstone damage evolution during triaxial compression with chemical corrosion[J]. International Journal of Rock Mechanics and Mining Sciences, 2004, 41(2): 181-192.
5. Qiao L P, Wang Z C, Huang A D. Alteration of mesoscopic properties and mechanical behavior of sandstone due to hydro-physical and hydro-chemical effects[J]. Rock Mechanics and Rock Engineering, 2016, 50(10): 255-267.
6. Li S G, Wu Y M, Huo R K, et al. Mechanical properties of acid-corroded sandstone under uniaxial compression[J]. Rock Mechanics and Rock Engineering, 2020, 54(10): 289-302.
7. Ge X R, Jiang Y, Lu Y D, et al. Experimental study on fatigue deformation characteristics of rock under cyclic loading[J]. Chinese Journal of Rock Mechanics and Engineering, 2003, 22(10): 1581-1585.
8. Zhou Z L, Cai X, Cao W Z, et al. Influence of water content on mechanical properties of rock in both saturation and drying processes[J]. Rock Mechanics and Rock Engineering, 2016, 49: 3009-3025.
9. Miao S J, Cai M F, Guo Q F, et al. Damage effects and mechanisms in granite treated with acidic chemical solutions[J]. International Journal of Rock Mechanics and Mining Sciences, 2016, 88: 77-86.
10. Yuan L, Yang K. Re-discussion on scientific problems and countermeasures for the utilization of abandoned mines[J]. Journal of China Coal Society, 2021, 46(1): 16-24.

Open Access This chapter is licensed under the terms of the Creative Commons Attribution-NonCommercial 4.0 International License (http://creativecommons.org/licenses/by-nc/4.0/), which permits any noncommercial use, sharing, adaptation, distribution and reproduction in any medium or format, as long as you give appropriate credit to the original author(s) and the source, provide a link to the Creative Commons license and indicate if changes were made.

The images or other third party material in this chapter are included in the chapter's Creative Commons license, unless indicated otherwise in a credit line to the material. If material is not included in the chapter's Creative Commons license and your intended use is not permitted by statutory regulation or exceeds the permitted use, you will need to obtain permission directly from the copyright holder.